Neurochemical dynamics of acute orofacial pain in the human trigeminal brainstem nuclear complex

de Matos, Nuno M P ; Hock, Andreas ; Wyss, Michael ; Ettlin, Dominik A ; Brügger, Mike

Abstract: The trigeminal brainstem sensory nuclear complex is the first central relay structure mediating orofacial somatosensory and nociceptive perception. Animal studies suggest a substantial involvement of neurochemical alterations at such basal CNS levels in acute and chronic pain processing. Translating this animal based knowledge to humans is challenging. Human related examining of brainstem functions are challenged by MR related peculiarities as well as applicability aspects of experimentally standardized paradigms. Based on our experience with an MR compatible human orofacial pain model, the aims of the present study were twofold: 1) from a technical perspective, the evaluation of proton magnetic resonance spectroscopy at 3 T regarding measurement accuracy of neurochemical profiles in this small brainstem nuclear complex and 2) the examination of possible neurochemical alterations induced by an experimental orofacial pain model. Data from 13 healthy volunteers aged 19-46 years were analyzed and revealed high quality spectra with significant reductions in total N-acetylaspartate (N-acetylaspartate + N-acetylaspartylglutamate) (-3.7%, p = 0.009) and GABA (-10.88%, p = 0.041) during the pain condition. These results might reflect contributions of N-acetylaspartate and N-acetylaspartylglutamate in neuronal activity-dependent physiologic processes and/or excitatory neurotransmission, whereas changes in GABA might indicate towards a reduction in tonic GABAergic functioning during nociceptive signaling. Summarized, the present study indicates the applicability of 1H-MRS to obtain neurochemical dynamics within the human trigeminal brainstem sensory nuclear complex. Further developments are needed to pave the way towards bridging important animal based knowledge with human research to understand the neurochemistry of orofacial nociception and pain.

DOI: https://doi.org/10.1016/j.neuroimage.2017.08.078

DOI: https://doi.org/10.1016/j.neuroimage.2017.08.078

Accepted Manuscript

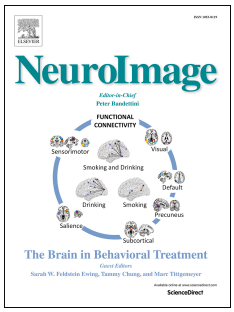

Neurochemical dynamics of acute orofacial pain in the human trigeminal brainstem nuclear complex

Nuno M.P. de Matos, Andreas Hock, Michael Wyss, Dominik A. Ettlin, Mike Brügger

PII: S1053-8119(17)30725-5

DOI: 10.1016/j.neuroimage.2017.08.078

Reference: YNIMG 14309

To appear in: *NeuroImage*

Received Date: 27 April 2017

Revised Date: 28 August 2017

Accepted Date: 30 August 2017

Please cite this article as: de Matos, N.M.P., Hock, A., Wyss, M., Ettlin, D.A., Brügger, M., Neurochemical dynamics of acute orofacial pain in the human trigeminal brainstem nuclear complex, *NeuroImage* (2017), doi: 10.1016/j.neuroimage.2017.08.078.

Neurochemical dynamics of acute orofacial pain in the human trigeminal brainstem nuclear complex

Nuno M. P. de Matos[1,2,5*], Andreas Hock[3,4,5], Michael Wyss[3], Dominik A. Ettlin[1], Mike Brügger[1,3]

[1]Center of Dental Medicine, University of Zurich, Zurich, Switzerland
[2]Institute for Complementary and Integrative Medicine, University Hospital Zurich and University of Zurich, Zurich, Switzerland
[3]Institute for Biomedical Engineering, University of Zurich and ETH Zurich, Zurich, Switzerland
[4]Philips Healthcare, Hamburg, Germany
[5]Contributed equally to the study

Correspondence:

Nuno M. P. de Matos
nuno.pratesdematos@usz.ch

Abstract

The trigeminal brainstem sensory nuclear complex is the first central relay structure mediating orofacial somatosensory and nociceptive perception. Animal studies suggest a substantial involvement of neurochemical alterations at such basal CNS levels in acute and chronic pain processing. Translating this animal based knowledge to humans is challenging. Human related examining of brainstem functions are challenged by MR related peculiarities as well as applicability aspects of experimentally standardized paradigms.

Based on our experience with an MR compatible human orofacial pain model, the aims of the present study were twofold: 1) from a technical perspective, the evaluation of proton magnetic resonance spectroscopy at 3 Tesla regarding measurement accuracy of neurochemical profiles in this small brainstem nuclear complex and 2) the examination of possible neurochemical alterations induced by an experimental orofacial pain model.

Data from 13 healthy volunteers aged 19 to 46 years were analyzed and revealed high quality spectra with significant reductions in total *N*-acetylaspartate (*N*-acetylaspartate + *N*-acetylaspartylglutamate) (-3.7%, p = 0.009) and GABA (-10.88%, p = 0.041) during the pain condition. These results might reflect contributions of N-acetylaspartate and N-acetylaspartylglutamate in neuronal activity-dependent physiologic processes and/or excitatory neurotransmission, whereas changes in GABA might indicate towards a reduction in tonic GABAergic functioning during nociceptive signaling.

Summarized, the present study indicates the applicability of ^{1}H-MRS to obtain neurochemical dynamics within the human trigeminal brainstem sensory nuclear complex. Further developments are needed to pave the way towards bridging important animal based knowledge with human research to understand the neurochemistry of orofacial nociception and pain.

Keywords: proton magnetic resonance spectroscopy, brainstem, trigeminal brainstem sensory nuclear complex TBSNC, region-specific neurochemistry, N-acetylaspartate NAA, GABA, dental pain, orofacial pain, human pain model

Introduction

Pain in general and orofacial pain in particular are complex multifaceted phenomena encompassing sensory, affective, cognitive and motor processes. Worldwide costs, suffering and psychosocial distress especially in chronic forms are immense (Maixner et al., 2011; Murray and Lopez, 2013). Related brain mechanisms have been disentangled up to a certain degree, with several (predominantly cortical) areas being involved in decoding specified information from the underlying pain cascade (Peyron et al., 2000; Wager et al., 2013; Denk et al., 2014). In contrast to these quite well described (pain related) neuronal correlates, the brainstem still remains scarcely characterized, particularly in humans (Beissner and Baudrexel, 2014).

As neuronal gate to and from the cortex, this structure is involved in a multitude of vital functional processes and of crucial importance for our daily survival. The functional spectrum of this area covers co-control of breathing, sleep-wake rhythms, blood pressure, heart rate, pain modulation and even higher cognitive and psychological functions (Sessle, 2005; Fairhurst et al., 2007; Hurley et al., 2010).

Listed as one of the most prevalent pain conditions, orofacial pain seems strongly associated with maladaptive brainstem processing (Sessle, 2000; Maixner et al., 2011). The collective term “orofacial pain” encompasses a variety of pain types perceived in the face, jaw and oral cavity including acute (eg. dental pain) and chronic conditions (eg. trigeminal neuralgia; trigeminal neuropathic pain; burning mouth syndrome; temporomandibular disorders) (Zakrzewska, 2013). One commonality of these different pain types is that their nociceptive information is exclusively transmitted to the brain via the trigeminal brainstem sensory nuclear complex (TBSNC) (Sessle, 2000). This intricate nuclear cluster represents the first relay station in the brain for peripheral somatosensory afferents from the trigeminal nerve (and to a smaller extent from the facial and glossopharyngeal nerves) (Sessle, 2000; DaSilva and DosSantos, 2012). It consists of three nuclei ranging from the mesencephalon down to the cervical dorsal horn, namely: mesencephalic, principal and spinal trigeminal nucleus (Nieuwenhuys et al., 2008). The spinal trigeminal nucleus (Sp5) is further subdivided into three subnuclei in a rostral to caudal fashion: Subnuclei pars oralis, pars interpolaris and pars caudalis (Dubner and Bennett, 1983; Beck et al., 1997; Nieuwenhuys et al., 2008). The TBSNC (Sp5 in particular) receives nociceptive signals from the ipsilateral site of the face and mouth via Aδ and C-fibers and forwards them via 2nd-order neurons to the contralateral

ventral posteromedial nucleus (VPM) of the thalamus from which the stimuli are further projected to several cortical structures (Nieuwenhuys et al., 2008).

Based on animal studies, cellular and neurochemical alterations in the TBSNC were suggested being crucially involved in processing acute pain as well as in maladaptation mechanisms leading to pain chronification. Neurochemicals released in the TBSNC by afferents, interneurons and (pain) modulatory pathways – most notably GABA, 5-HT and opioids – alter the processing of nociceptive input on that basal CNS level (Sessle, 2000). Exemplary are various investigations demonstrating changes in GABAergic neurotransmission associated with trauma, inflammation and partial deafferentation (Sessle, 2000; Viggiano et al., 2004; Takeda et al., 2011). Additionally, evidence is given by chronic neuropathic pain models. Using a constriction injury model of the rat infraorbital branch of the trigeminal nerve (CCI-ION), only baclofen (a $GABA_B$-receptor agonist) but not carbamazepine, morphine or tricyclic antidepressants were able to reduce the allodynia-like behavior (Idänpään-Heikkilä and Guilbaud, 1999). Using a similar model, Martin et al. (2010) found a decrease in GAD65 immunoreactivity in the caudal nucleus of the Sp5 suggesting a disruption in GABA-mediated inhibitory circuits.

Few human neuroimaging studies addressed the specific functional/anatomical contributions of the TBSNC in acute and chronic orofacial pain by applying functional magnetic resonance imaging (fMRI) (DaSilva et al., 2002), diffusion tensor imaging (DTI) and voxel-based morphometry (VBM) (Wilcox et al., 2015). However, none of the performed neuroimaging studies provided insights regarding neurochemical alterations in the human TBSNC thus corroborating some results provided by animal studies. But this question could be addressed by proton magnetic resonance spectroscopy (^{1}H-MRS), a powerful method able to simultaneously quantify neurochemical compounds in a defined brain region. Typically measured neurochemicals provide for example information about neuronal density and viability (*N*-acetylaspartate), energy metabolism (creatine/phosphocreatine), membrane turnover and integrity (choline), antioxidant status (glutathione), glial cell proliferation (Myo-inositol) or neurotransmission (Glutamate, GABA, N-acetyl-aspartyl-glutamate)(Stagg, 2013). Theoretically, ^{1}H-MRS allows observing neurochemical processes and alterations associated with acute and chronic (orofacial) pain conditions within relevant brainstem nuclei. Thus a bridge from human research to the animal studies on TBSNC might be in reach.

However, in-vivo measurements on brainstem levels face a series of significant challenges as technical, structural and physiological characteristics of the brainstem and spinal cord impede

proper MR acquisitions. Blood flow in adjacent arteries/venes and CSF pulsation in and around the brainstem induce inhomogeneity in the static magnetic field (B_0) thus causing frequency shifts resulting in poor spectral resolution (Brooks et al., 2013; Beissner and Baudrexel, 2014; Hock et al., 2013). Furthermore, the signal obtained by ^{1}H-MRS is in general very minute, demanding large measurement volumes (usually voxel sizes of 8 ml) in order to achieve sufficient signal-to-noise ratios (SNR) in a reasonable acquisition time (Kreis, 2004; de Matos et al., 2016). But, measuring the TBSNC with the adequate anatomical and functional specificity demands smaller voxel sizes and hence requires adaptations towards long acquisition times. Those, in turn enhance the likelihood for temporal changes in the B_0 field caused by subject motion and B_0 drifts resulting in frequency and phase shifts between single free induction decays (FIDs). All these facets hamper spectral quality aspects and require careful planning and adequate measurement strategies (Hock et al., 2013c).

In this feasibility study, we provide a brainstem optimized ^{1}H-MRS sequence and data post processing scheme in combination with a reliable experimental dental pain model in healthy volunteers. The following two questions were pursued: 1) ^{1}H-MRS measurability aspects of a small brainstem area from a technical perspective and 2) possible alterations in the neurochemical milieu induced by experimental dental pain.

Materials and Methods:

The present study was conducted from March 2015 to December 2015 according to the Declaration of Helsinki and was approved by the local ethics committee.

Subjects:

26 healthy males (mean age: 27.35 ± 6.84, range: 19-46) were recruited for the study. Inclusion criteria required the test tooth (right upper canine) to be vital, caries free, sensorically intact and free of previous dental treatments. Exclusion criteria were psychiatric and neurologic diseases, regular pain medication intake, pain syndromes, claustrophobia and general contra-indications for MR. No female volunteers were recruited due to possible variability in pain perception caused by menstrual cycle associated variation in hormonal levels (Wiesenfeld-Hallin, 2005).

All subjects received detailed information about the experimental procedure, aim of the study and provided their written informed consent before any procedure was performed. Subjects were instructed not to consume alcohol, analgesic medication and other drugs 24h before the start of the MR experiment and to be fed before participation. Participants were explicitly informed to have the possibility to terminate participation and withdraw from the study at any time. They were financially compensated (40 Swiss francs/hour) for the effective time of participation.

From the initial 26 recruited participants, 8 were excluded after the test session due to insufficient and/or inconstant pain intensity perception; therefore 18 subjects were included in the study. Two subjects had to be excluded due to spectral artifacts and two others due to insufficient spectral resolution ($FWHM_{NAA}$ > 10Hz). An additional subject had to be excluded due to strong movements during the experimental conditions, resulting in a total of 13 (mean age: 27.69 ± 7.89, range: 19-46) data sets for analysis.

Dental stimulation setup:

Dental stimulation was administered to the right upper canine. For this purpose, individual dental splints with non-ferromagnetic stainless steel electrodes embedded directly at the center of labial and palatal surfaces were fabricated. To reduce electrical resistance, small portions of hydrogel (size ca. 3x3mm) covering the electrodes were applied before splint insertion.

In addition to the tooth stimulating electrodes, a small 2 MΩ resistor (surface-mount device, SMD, KOA Corporation, Tokyo, Japan) was placed on the left side of the dental splint over the second left incisor tooth and sealed with Blu-Mousse (thixotropic vinyl polysiloxane; Parkell, Edgewood, USA). This resistor served as "dummy tooth" enabling running of the stimulation procedure during the baseline measurements without evoking sensory perceptions. This approach allowed for identical conditions during baseline and pain ^{1}H-MRS measurements.

For details regarding splint fabrication and stimulation equipment specs, please see Gutzeit et al., 2013.

Psychophysical testing and familiarization:

Subjects were invited to a test session 1-2 weeks prior to the MR-experiment. The aim of this preceding visit was fourfold: 1) Check of inclusion/exclusion criteria, 2) manufacturing of the dental splint, 3) psychophysical testing of the subjects' sensory and pain thresholds and 4) familiarization of the participant with the dental stimulation procedure and equipment.

The psychophysical testing consisted of the administration of electrical pulses of 1 ms duration with linearly increasing electrical currents and randomized inter-stimulus-intervals (ISI) 5-8s long. The procedure started at an imperceptible intensity of 1 mA; the intensity was then increased in steps of 1 mA. Thresholds for sensory detection (SDT), pain detection (PDT), and a stimulus intensity corresponding to the subjects' individual rating of 4-5 (moderately painful) on a NRS were obtained. 4-5 was the target pain intensity for the pain stimulation condition in the MR-experiment. Subjects indicated the SDT, PDT and 4-5 by hand signs. This procedure was repeated 3 times to assure the stability of individual sensory thresholds as well as account for novelty effects and potential initial feelings of uneasiness associated with the dental stimulation.

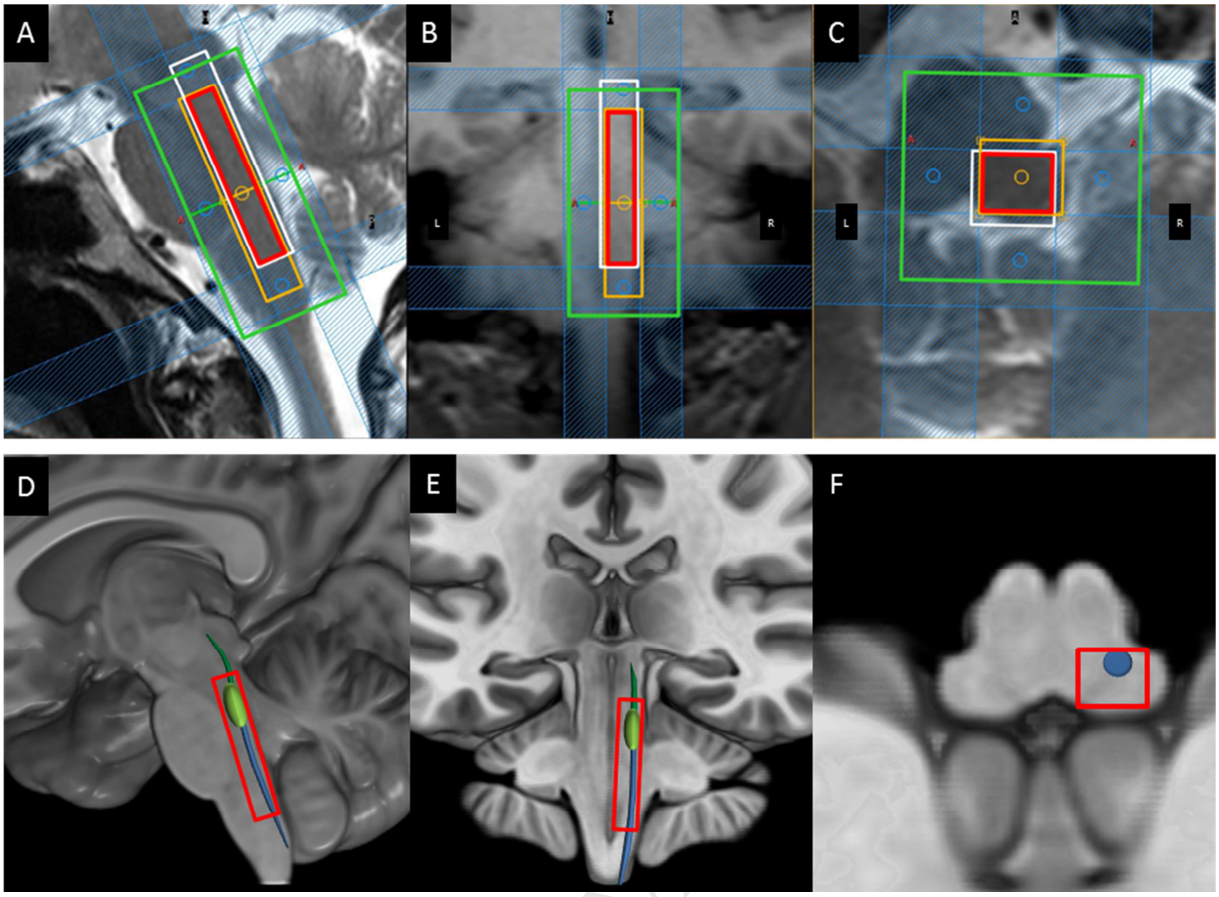

Figure 1: Panels A-C illustrate the MRS voxel placement on sagittal (A), coronal (B) and transversal (C) anatomical images. Orange and white boxes represent the acquisition volumes of lactate (orange) and myo-inositol (white) which are shifted relative to each other due to the chemical shift artifact. This artifact is reduced by the use of inner-volume saturation (IVS) bands. The red box corresponds to the resulting excitation volume generating the MRS signal. In addition, the shim box is represented by the green box. Panels D-F illustrate the position of the excitation volume (red) in relation to the schematically represented TBSNC with the associated mesencephalic (dark green), primary (light green) and spinal trigeminal nuclei (blue) on sagittal, coronal and transversal images.

Experimental Procedure:

At the beginning of the MR-experiment, psychophysical testing (procedure identical to the test session) was performed and the SDT, PDT and intensity of 4-5 was evaluated outside the scanner to test the participants' current perceptual characteristics.

The subjects were then positioned in the 3-Tesla MR unit (Philips Healthcare, Best, The Netherlands) in a supine position. Since small voxel dimensions were applied in an anatomical localization difficult to investigate, it was crucial to keep head movements at a minimum. Multipad positioning cushions (Pearltec AG, Schlieren / Zurich, Switzerland) were used for this purpose. Two were bilaterally placed between the temple and the coil, and a third was positioned under the participant's neck/occipital head. Subjects adjusted the cushion

inflation for optimal comfort which is essential considering the extended measurement durations. Participants were instructed to press the alarm button in case of discomfort caused by the head fixation system.

After acquisition of anatomical sequences and placement of the MRS-voxel, the baseline MRS measurement was obtained. During this baseline condition, dummy stimulation was applied. Psychophysical testing was then repeated inside the scanner to adjust, if necessary, the electrical current strength evoking a 4-5/10 pain intensity. Prior to the painful measurement sequence, correct voxel placement was verified on another set of anatomical images and adjusted if necessary. Electrical stimulation during the baseline and pain stimulation block consisted of 128 short pulses (1 ms, identical characteristics as during the psychophysical testing) administered with an ISI of 10-12.5s (block duration: approx. 21

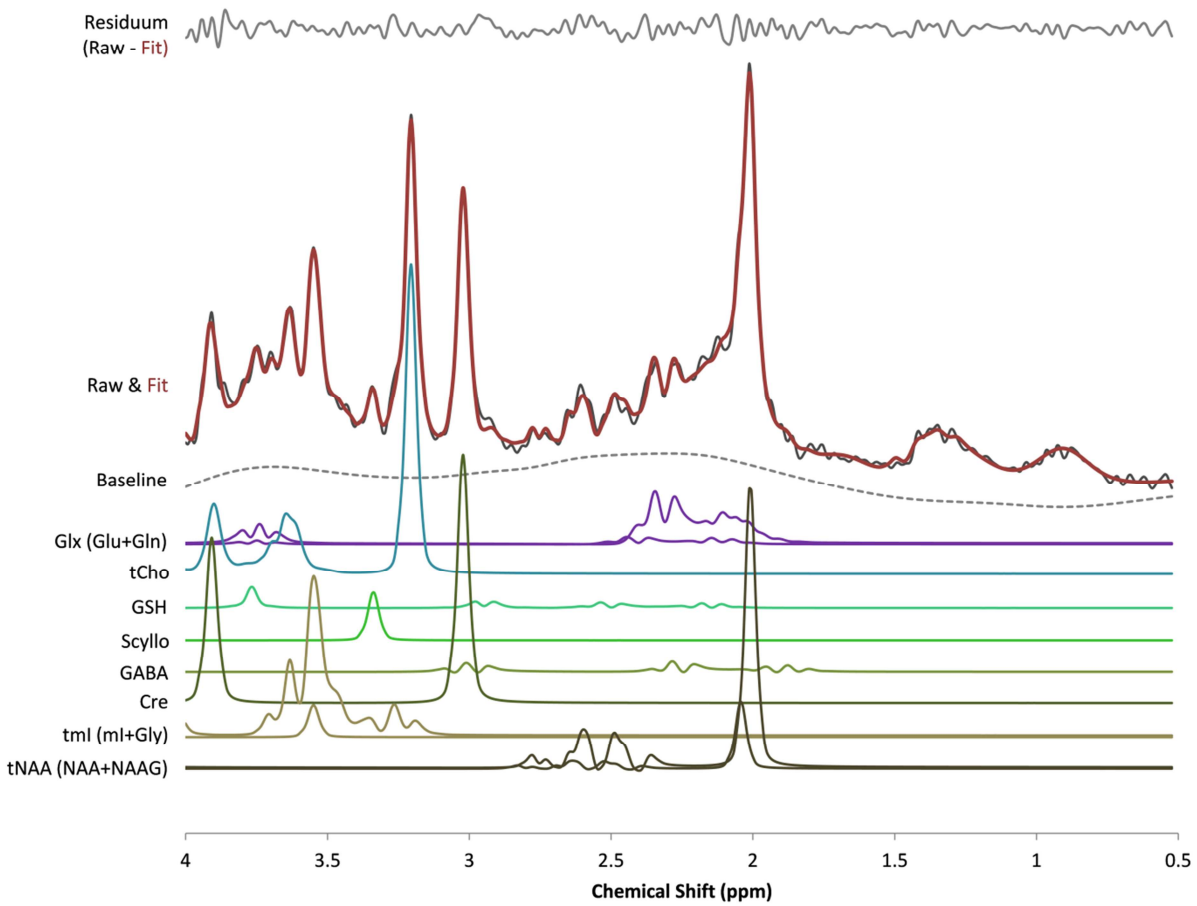

Figure 2: Exemplary spectrum fitted with LCModel. The fitted spectum (red) is superimposed on the raw spectrum (grey). The difference of raw and fitted spectrum is displayed by the residuum which is an indicator for the goodness-of-fit. The spectral baseline is delineated by the dashed grey line. The fits of the reported neurochemicals are displayed below the baseline.

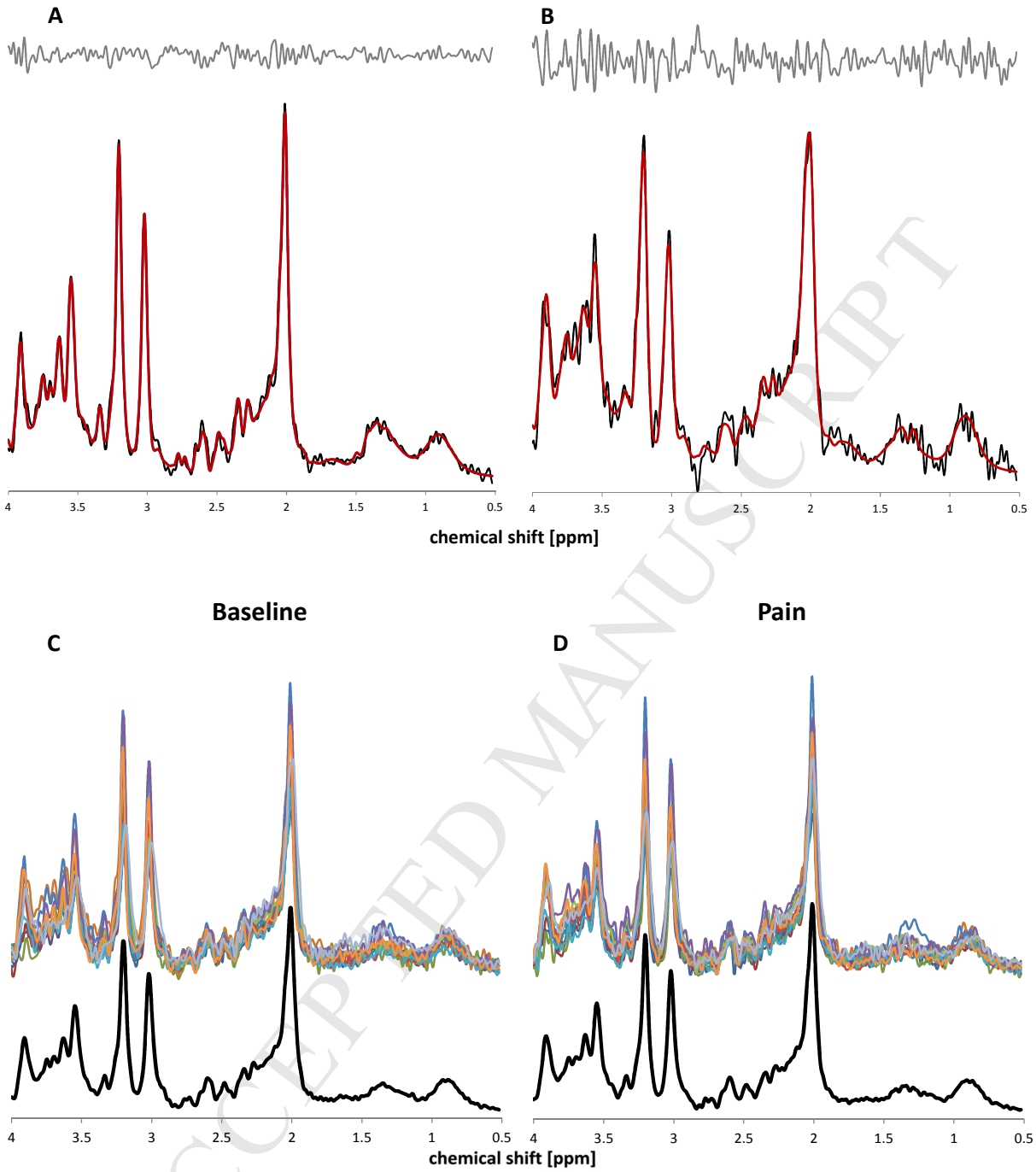

Figure 3: Overview of the spectral quality range of included spectra. Quality estimates (from LCModel) of the best spectrum (A) were: SNR = 23, Linewidth = 4.85 Hz. Estimates of the worst (B) were: SNR = 12, Linewidth = 7.79 Hz. Mean spectral quality over all spectra: SNR = 19.08, Linewidth = 6.41 Hz. Panels C and D illustrate the spectral variability as overlay of all 13 included spectra (colored lines) with the corresponding averaged spectrum (black) for the baseline (C) and pain (D) condition.

minutes). Previous work demonstrates that the applied dental stimulation paradigm is not prone to sensitization and habituation effects during long measurement periods (Brügger et al., 2012). The total duration of the MR measurement was approx. 60 min.

MR protocol

The integrated body coil was used for transmission (maximum B_1 = 13.5 μT); a receive-only 8 channel head coil array (Philips Healthcare, Best, NL) was applied for signal reception. Anatomical high-resolution T2-weighted turbo spin-echo sequences were performed in axial and sagittal orientations (TR/TE = 3000/120; Flip-angle = 90°; voxel size 0.8x1x3.2mm^3) to ensure precise voxel planning and positioning.

For the MR spectra acquisition, an inner-volume saturated (IVS)(Edden et al., 2006; Hock et al., 2013), non-water suppressed PRESS (point-resolved spectroscopy) sequence (TR/TE = 2500/32 ms; data points = 1024; sample frequency = 2000 Hz; readout duration = 512 ms; number of averages = 512) was used via the metabolite cycling (MC) technique (MC-PRESS) (Dreher and Leibfritz, 2005; Hock et al., 2013). This enables a simultaneous recording of water and neurochemical signals, by adding or subtracting consecutively acquired echoes modulated via alternate up- or downfield inversion pulses which do not affect the water signal (Dreher and Leibfritz, 2005; Hock et al., 2013). Therefore, MC-PRESS allows the acquisition of high SNR water-peaks from single FIDs, permitting frequency alignment, phase and eddy current correction before averaging of neurochemical spectra. Hence, MC-PRESS provides the potential to reduce frequency shifts caused by pulsatile effects of blood vessels/CSF and B_0 drifts. Furthermore, the simultaneous acquisition of both water and neurochemical signals means that both are subject to the same MR-specific and physiologic influences thus optimizing the use of the water peak as an internal reference during neurochemical quantification.

To optimally cover the region of interest, the MRS voxel was carefully placed along the transition zone to the 4th ventricle. Important to note: due to individual shapes and contours of the volunteers' brainstem, the placements were adjusted to avoid contamination of the MRS voxel with CSF from the 4th ventricle, central canal and cisterna magna. The voxel was placed on the ipsilateral side in reference to the stimulated tooth using following dimensions: 37.6 x 8.5 x 7.6 mm (2.4ml, Fig. 1).

MRS data post processing

MRS data were post-processed according to Hock et al. (2013; 2016). The individual 512 FIDs were truncated after 100ms and zero-filled to 1024 points, followed by frequency alignment, phase and eddy current correction of individual FIDs before averaging. These

steps were performed using in-house scripts running on MATLAB 2013b (MathWorks, Natick, MA, USA).

In case of a significant mismatch of spectral linewidth estimates between both conditions, filtering by means of an exponential multiplication was performed to minimize systematic errors in neurochemical quantification. This approach prevents false neurochemical differences between the conditions (Mangia et al., 2007). The correction was done by matching the water peak linewidth to the water peak linewidth of the pain spectrum. Individual filter parameters were chosen to ensure the best match possible for each participant.

Quantification of Neurochemicals

Neurochemicals were quantified with LCModel (Provencher, 1993) using a set of basis spectra which were simulated using the GAMMA Simulation Package (Smith et al., 1994). The basis set included the following components: *N*-acetyl aspartate (NAA), *N*-acetyl-aspartyl glutamate (NAAG), glycerophosphocholine (GPC), phosphocholine (PCh), creatine (Cre), myo-Inositol (mI), glycine (gly), alanine (Ala), ascorbic acid (Asc), aspartate (Asp), ethanolamine and phosphorylethanolamine (PE), glutamine (Gln), glutamate (Glu), glutathione (GSH), glucose (Glc), γ-aminobutyric acid (GABA), lactate (Lac), taurine (Tau) and scyllo-inositol (sI). The chemical shift range was set to 4.0-0.5 ppm. Following neurochemicals with strongly overlapping spectra were combined to one single spectrum: Glu + Gln = Glx, GPC + PCh = tCho, mI + Gly = tmI and NAA + NAAG = tNAA.

With respect to neurochemical related inclusion criteria, we followed the suggestions provided by De Graaf (2007): Neurochemicals with CRLB<10% count as measured with sufficient precision, neurochemicals with CRLB <20-30% should be considered with caution whereas neurochemicals with CRLB >30% are deemed unreliable and should therefore be excluded from the analysis. Hence, the following neurochemicals were included: tNAA, tCho, tmI, Cre, Glx, GSH, Scyllo and GABA.

We decided to use water (from the simultaneously acquired water spectra) as internal reference instead of Cre due to the following reasons:

1. Previous pain MRS studies observed significant alterations in Cre concentrations (see Gutzeit et al., 2013).

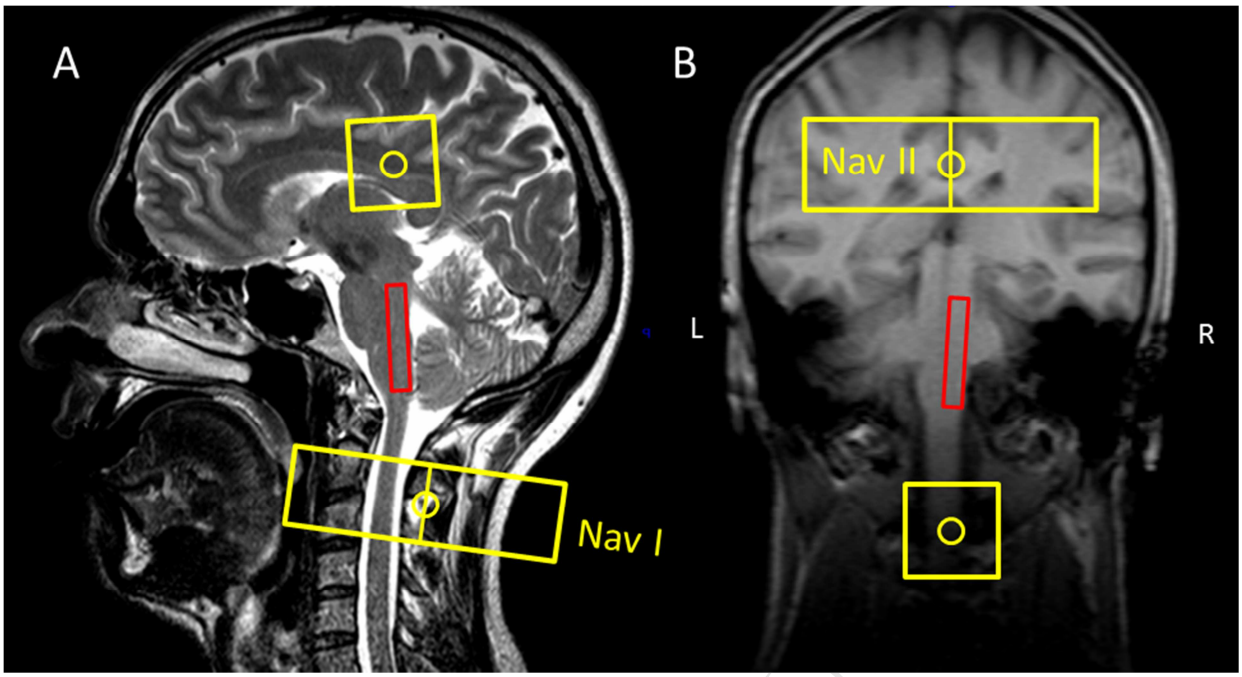

Figure 4: Placement of the two navigators (orange) shown on sagittal (A) and coronal (B) images. , The lower navigator (Nav I) measured movement in the anterior-posterior axis, he upper navigator (Nav II) measured movement in the left-right axis. The red box corresponds to the MRS excitation volume.

2. Reduced sensitivity due to combined quantification errors of Cre and the other neurochemicals (resulting in higher variation).

3. Unspecific Cre signal changes could either under- or overestimate "true" effects in other neurochemicals evoked by the experimental conditions.

Movement

Two navigator sequences were performed during both conditions. This procedure enables two different approaches to reduce the impact of motion on the neurochemical data: Firstly, real time feedback to instruct the volunteers not to move and secondly, rejecting data sets with excessive levels of motion.

Navigator sequences were carried out in the dead time before the inner-volume saturation (IVS) pulses of each single MRS acquisition (pencil-beam excitation with radius r = 30mm and length l = 100mm; flip-angle = 15°, acquisition duration = 2.9ms) (Hock and Henning, 2016).

The first navigator (Nav I, anterior-posterior axis) was positioned ventral to the MRS voxel perpendicularly oriented to the medulla. The second one (Nav II, left-right axis) was placed dorsally to the MRS-voxel covering corpus callosum and occipital areas (Fig. 4).

Navigator positions were extracted from the raw MR data using MRecon (GyroTools, Zurich, Switzerland). The extracted movement data was used for the calculation of relative movement during individual scans using the first navigator acquisition as reference. A gating window of ±1mm was used to identify echoes associated with significant movement. Navigator data demonstrating excessive noise were excluded (See excluded data sets in supplementary material).

Spectra from individual participants were excluded from the analysis based on their movement estimates if more than 10% of the individual spectral acquisitions were shifted outside the gating window.

Statistical analysis

SPSS 22 (IBM Corp., Armonk, NY, USA) was used to perform the statistics; the significance threshold was set at $p < 0.05$. First, data were tested for normal distribution by means of the Shapiro-Wilk test. Differences between both experimental conditions regarding neurochemical concentrations were tested using a paired t-test, whereas comparison of SNR

Table 1: Estimates of spectral quality and fitting errors (CRLB) of the included spectra from the baseline and pain conditions. In addition, inter-scan variation estimates are presented as coefficients of variation (CV). Values are reported as means ± SD.

	Baseline	Pain	P
Spectral quality:			
$FWHM_{NAA}$[Hz] [a]	6.6 ± 1.7	5.8 ± 1.6	**0.008**
$FWHM_{NAA}$[Hz] [b]	6.5 ± 1.6	6.3 ± 1.4	0.611
SNR_{NAA}	19.1 ± 2.7	19.1 ± 2.3	1.000
CRLB [%]:			Inter-scan CV [%]:
tCho	3.2 ± 0.7	3.0 ± 0.6	2.7 ± 1.6
tNAA	2.8 ± 0.4	3.2 ± 0.8	3.4 ±2.1
tmI	3.4 ± 0.5	3.3 ± 0.5	2.4 ± 2.3
Cre	3.4 ± 1.1	3.3 ± 0.5	2.6 ± 2.0
Glx	9.3 ± 1.7	11.0 ± 5.2	12.6 ± 12.7
Scyllo	18.6 ± 7.4	19.3 ± 7.3	13.72 ± 10.6
GSH	21.9 ± 7.8	23.8 ± 11.3	25.3 ± 26.5
GABA	23.4 ± 6.3	26.5 ± 8.4	16.1 ± 15.9

[a] Linewidth estimates provided by LCModel without linewidth-matching of the water peaks
[b] Linewidth estimates provided by LCModel with linewidth-matching of the water peaks (by means of exponential filtering)

Table 2: Water peak area (mean ± SD; area under the curve, AUC) and absolute neurochemical concentrations (mean ± SD; institutional units) of included metabolites from both conditions. Significance levels of the paired t-test between both conditions are represented under p.

	Baseline	Pain	Abs. Change	Rel. Change [%]	p
$H2O_{AUC}$	47.48 ± 4.75	47.58 ± 4.39	0.10 ± 0.61	0.29 ± 1.52	0.580
tCho	6.50 ± 0.75	6.44 ± 0.75	-0.06 ± 0.30	-0.78 ± 4.50	0.515
tNAA	22.89 ± 2.54	22.01 ± 2.35	-0.87 ± 1.01	-3.70 ± 4.11	**0.009**
tmI	21.73 ± 2.70	21.55 ± 2.25	-0.18±1.05	-0.50 ± 4.73	0.552
Cre	15.31 ± 1.56	15.13 ± 1.56	-0.18 ± 0.74	-1.07±4.51	0.404
Glx	19.28 ±4.09	18.17 ± 5.55	-1.10 ± 3.81	-3.67 ± 25.35	0.317
Scyllo	1.28 ± 0.44	1.18 ± 0.41	-0.10 ± 0.26	-3.93 ± 22.73	0.206
GSH	3.57 ± 1.33	3.35 ± 1.42	-0.23 ± 1.57	2.02 ± 44.85	0.612
GABA	6.29 ± 1.79	5.40 ± 1.63	-0.89 ± 1.41	-10.88 ± 24.47	**0.041**

and linewidth was tested using a Wilcoxon signed-rank. In order to estimate reproducibility, inter-scan variability (variability between baseline and pain condition for each participant) was estimated by means of coefficient of variation (CV, calculated as SD/Mean*100).

Results

Data quality

Mean spectral quality and fitting error estimates for both conditions are shown in table 1. Linewidth estimates provided by LCModel differed significantly between both conditions (Z = -2.670, p = 0.008). In order to minimize linewidth differences, individual baseline spectra were filtered resulting in negligible linewidth differences (Z = -0.509, p = 0.611). Mean SNR was 19.1 for both conditions and thus not significant (Z = 0.000, p = 1.000). The good data quality is also reflected by the low CRLB over all spectra and all subjects (Baseline: 9.6%; Pain: 11.1%). As a consequence, resulting inter-scan CV were low with mean CV of 9.85% over all participants and included neurochemicals (see Table 1).

Table 3: Movement analysis results. Mean displacement (±SD), and the mean percentage of MRS acquisitions (Range) exceeding the gating-window (±1mm). Significance levels of the wilcoxon-test between both conditions are represented under p.

Group analysis	Nav I (anterior-posterior axis)			Nav II (left-right axis)		
	Baseline	Pain	p	Baseline	Pain	p
Mean [mm]	-0.19 ±0.25	-0.25 ± 0.22	0.60	-0.27 ± 0.28	-0.23 ± 0.26	0.42
Echoes > ±1mm [%]	0.50 (0-3.13)	0.90 (0-7.81)	0.55	0.57 (0-4.30)	1.05 (0-9.57)	1.00

Excluded Participant	Nav I		Nav II	
	Baseline	Pain	Baseline	Pain
Mean[mm]	-0.41	-1.50	-0.07	-0.19
Echoes > ±1mm [%]	0.00	**73.83**	0.00	0.00

Movement

Two movement datasets from navigator 2 had to be excluded due to excessive noise, resulting in a complete data set of 13 movement profiles for navigator 1 (anterior-posterior, AP) and 11 movement profiles for navigator 2 (left-right, LR; Illustrations of the individual movement profiles are provided in the supplementary material). Spectra from one participant had to be excluded due to a significant drift movement in the anterior-posterior direction.

The movement quantification results are summarized in table 3. The overall movement was negligible with mean displacements of -0.22 mm (AP) and -0.25 (LR). Accordingly, the percentages of navigator echoes exceeding displacements of ±1mm were minute with mean percentages of 0.70% (AP) axis and 0.81% (LR). No significant differences were observed in mean displacement magnitudes between baseline and pain conditions for Nav I ($Z = 0.52$, $p = 0.60$) and Nav II ($Z = 0.80$, $p = 0.42$). In the same vein, the count of single navigator echoes lying outside gating window were also not significant between the baseline and pain condition for both navigators (Nav I: $Z = -0.60$, $p = 0.55$; Nav II: $Z = 0.00$, $p = 1.00$).

Neurochemical concentrations:

Table 2 shows absolute neurochemical concentrations and the resulting changes with corresponding paired t-test results. Figure 2 graphically illustrates the intra-individual neurochemical differences as boxplots. tNAA and GABA revealed significant alterations

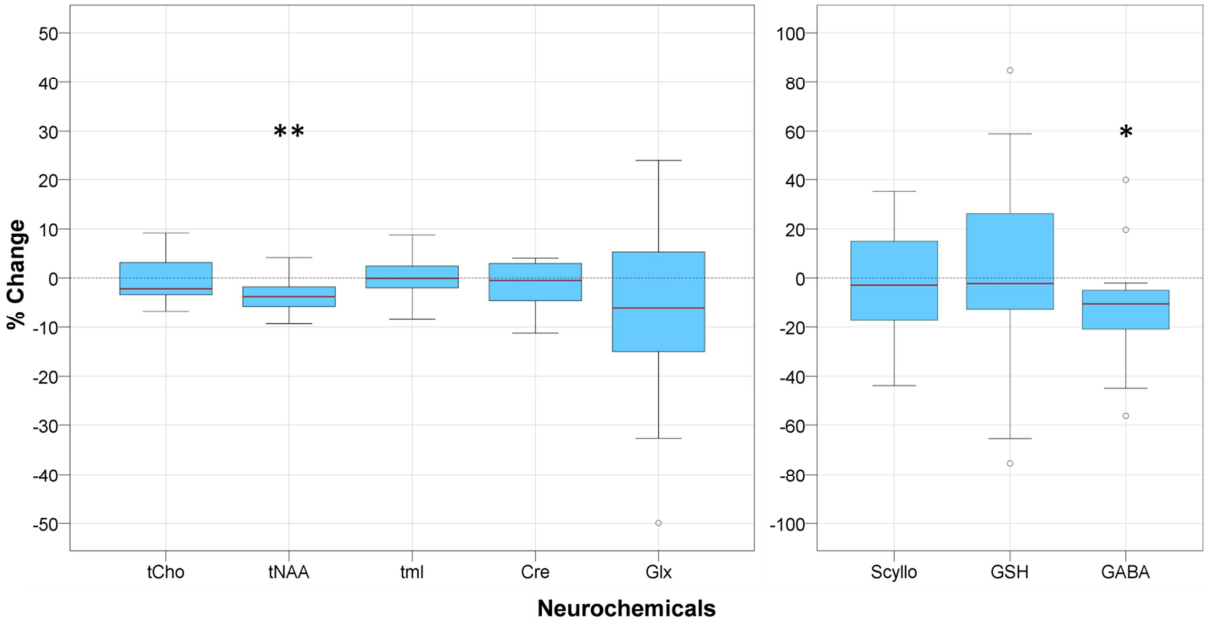

Figure 5: Boxplots of the percent changes in neurochemical concentrations between baseline and pain condition. tNAA and GABA showed a statistically significant reduction during pain stimulation. *p<0.05; **p<0.01

during the pain condition. tNAA showed the most significant differences with a consistent drop during pain (T = 3.130(12); p = 0.009). Also GABA demonstrated a significant concentration drop during pain (T = 2.286(12); p = 0.041).

Discussion

In the present study, neurochemical changes within the human TBSNC during experimental orofacial pain were assessed by brainstem-optimized functional ^{1}H-MRS. To our knowledge, this is the first human study which quantified neurochemical alterations at anatomically distinct brainstem level in response to experimental nociception. The combination of MC-PRESS ^{1}H-MRS-sequences and dedicated spectral post-processing enabled the acquisition of high quality spectra in spite of the present technical challenges inherent to the brainstem, long measurement times and small voxel dimensions. Eight neurochemicals were quantified with good reproducibility as indicated by overall low CRLBs and inter-scan CV (Table 1). From these eight neurochemicals, significant decreases were observed for tNAA and GABA during the pain application.

Mechanisms underlying NAA and NAAG decreases with an emphasis on nociception

NAA is one of the most abundant neurochemicals in the human nervous system reaching high concentrations of approx. 10mM (Moffett et al., 2007). In ^{1}H-MRS, this neurochemical is typically represented by the highest peak in the spectrum which originates from three nearly equivalent methyl hydrogen atoms on the acetate group resonating with a frequency shift of 2.02 ppm relative to the MRS standard tetramethylsilane (De Graaf, 2007). NAA is specific to neurons, being predominantly synthesized in neuronal mitochondria from aspartate and acetyl-coenzyme A by the enzyme L-aspartate N-acetyltransferase (Asp-NAT) (Stagg, 2013). NAA synthesis has been shown to be coupled to oxygen consumption and adenosine triphosphate (ATP) production, thus linking NAA to mitochondrial activity and associated neuronal energy metabolism (Benarroch, 2008). NAA counts as a reliable marker of neuronal health and integrity (Rae, 2014). Pursuant to, a variety of clinical conditions demonstrate transient or permanent decreases, confirmed in stroke, Alzheimer's disease, epilepsy, brain tumors, multiple sclerosis, schizophrenia, chronic low back and orofacial pain (Moffett et al., 2007; Benarroch, 2008; Gussew et al., 2011; Gustin et al., 2011). These results point towards an indubitably important role of NAA in those pathological conditions. However, it should be emphasized that its utility as marker for general neuronal health is primarily based on empirical evidence and not on a profound understanding of its specific neuronal functions, in particular during neuronal activity (Moffett et al., 2007; Stagg, 2013; Rae, 2014).

A variety of functional roles of NAA have been suggested in animal and human research. Baslow and coworkers (Baslow, 2002; Baslow et al., 2007; Baslow et al., 2016) proposed that NAA might additionally function as molecular water pump (MWP), able of removing excess water produced by increased glucose respiration during neuronal activation. According to this hypothesis, NAA is actively transported to the extracellular space in conjuction with bound water molecules. Subsequently, NAA is catabolized by aspartoacyclase (ASPA) in oligodendrocytes, releasing the bound water molecules and thus allowing water removal from the extracellular space by astrocytes. Although intriguing, the MWP-theory remains hypothetical as to date no key transport protein has been identified. Another possible mechanism for a controlled release of NAA during neuronal activation has been suggested by experiments performed on organotypic hippocampal slices. Tranberg et al. (2004) observed a NAA release during a 20 min period after a transient 5 min activation of NMDA-receptors. Importantly, the NAA efflux was not due to potassium depolarization, but to a NMDA-mediated influx of Ca^{2+}.

Such NMDA-mediated releases of NAA could function as an activity-driven mechanism for metabolic water removal thus supporting neurophysiological processes proposed by Baslow et al. (Baslow, 2002). In addition, this NMDA-mediated release could constitute a regulation mechanism for axon-glial signaling, which has been proposed by others (Moffett et al., 2007).

Widely accepted is the role of NAA as precursor for *N*-acetylaspartylglutamate (NAAG), the highest concentrated neuropeptide in the human CNS (Benarroch, 2008). NAAG is synthesized in neurons from NAA and glutamate and is then synaptically (calcium mediated) released. NAAG is predominately converted by glutamate carboxypeptidase II (GCPII) located on the surface of astrocytes. GPCII hydrolyzes NAAG back to NAA and glutamate which are taken up by astrocytes. Glutamate is then converted to glutamine and transported back to neurons. NAA, however, is most likely released to the blood stream by astrocytes (Moffett et al., 2007).

It has been suggested that NAAG binds to the metabotropic glutamate receptor 3 (mGluR3) located on presynaptic endings thus enabling a modulation of neurotransmitter release (Zhao et al., 2001; Zhong et al., 2006). Due to the co-localization of NAAG with major neurotransmitters (including glutamate, GABA, acetylcholine and serotonin, dopamine and norepinephrine), it possibly modulates their release from synapses (Moffett et al., 2007). It has been further proposed that NAAG could function as modulatory pro-transmitter. In this view, NAAG would act as a glutamate carrier, releasing glutamate at sites where active GCPII enzymes are present, therefore promoting focal glutamatergic neurotransmission (Stagg, 2013).

Functional ^{1}H-MRS (fMRS) studies have been conducted in the past to investigate neurochemical dynamics of acute experimental pain processing in cortical regions (anterior/posterior insular cortex, pregenual anterior cingulate cortex) of healthy volunteers (Mullins et al., 2005; Kupers et al., 2009; Gussew et al., 2010; Gutzeit et al., 2011; Gutzeit et al., 2013). Indeed, none of the performed studies reported significant changes in tNAA. Most interestingly, Gutzeit et al. (2011, 2013) applied the identical stimulation paradigm to investigate acute dental pain processing in the insular cortex and neither observed significant alteration regarding tNAA.

What could be possible reasons for the discrepancy between the presented work and previous fMRS pain studies? On one hand, the TBSNC represents the first CNS relay area, processing "pure" somatosensory input, thus reflecting basic nociception in contrast to multifaceted

"pain" processing in cortical regions. And with respect to brainstem neurochemical characteristics and compositions, various features are evident compared to cortical regions, especially regarding NAA and NAAG. Based on animal studies it has been stated that Asp-NAT enzyme activity increases from rostral to caudal brain structures with brainstem and spinal cord exhibiting the highest activity levels (Truckenmiller et al., 1985; Moffett et al., 2007). Interestingly, the expression of NAAG has been suggested to follow an analogue rostral-to-caudal pattern, being present at highest concentrations in the brainstem and spinal cord (Moffett and Namboodiri, 2006; Lodder-Gadaczek et al., 2011). Considering the reports on the absence of a similar concentration gradient of NAA (Tallan, 1957; Miyake et al., 1981), the elevated levels of NAAG may be linked to higher NAA synthesis rates in brainstem structures. In parallel to high NAAG concentrations, high densities of GCPII enzymes and mGluR2/3 were documented for the Sp5 in animal immunocytochemistry studies (Slusher et al., 1992; Tang et al., 2001), both closely interacting with NAAG (Zhao et al., 2001; Zhong et al., 2006). Under the consideration of suggested interactions between GCPII and neuropathic pain (Zhang et al., 2002; Zhang et al., 2006; Yamada et al., 2012) and mGlu2/3 receptors involved in orofacial pain at brainstem levels (Tang et al., 2001), our results provide evidence regarding NAAG release and catabolism in acute nociceptive pain processing in the human TBSNC.

Altogether, the observed tNAA reduction during the pain condition may reflect enhanced nociceptive-related NAAG neurotransmission in the TBSNC. The released NAAG would be degraded by GCPII releasing glutamate and NAA. The subsequent removal of NAA would finally result in a reduction of NAA signals in the spectrum. Hence, such a nociception/pain associated involvement of NAAG in the TBSNC could result in the observed reductions of tNAA. Furthermore, as NMDA likely plays a major role in nociceptive processing within the TBSNC (Sessle, 2000), activated NMDA receptors (either by direct glutamate release or indirect via NAAG) possibly lead to NAA efflux, thus further reducing the observable amount of NAA in the MRS signal.

Mechanisms underlying GABA decreases with an emphasis on nociception

GABA has two main roles within the CNS: On one side, it acts as neuronal metabolite throughout the cytoplasm and reflects the largest pool of GABA (Stagg, 2013). On the other hand, it is best known as main inhibitory neurotransmitter in the CNS (Stagg et al., 2011a). It

binds to two main types of receptors, both widely distributed over the brain, namely the ionotropic receptors $GABA_A$ and metabotropic $GABA_B$. They are located pre/post and extrasynaptically, hence underlying its comprising role to extensively alter neural activation (Rae, 2014). GABA is thus involved in the modulation of a variety of physiological processes (motor control, pain, sleep) and is supposed to be dysfunctional in several pathological conditions (epilepsy, anxiety, wake-sleep disturbances, schizophrenia) as well as developmental and neurodegenerative disorders (Rae, 2014).

However, to describe distinct roles of GABA within this functional diversity is challenging. Exemplary is the study of Jasmin et al. (2003). By selectively modulating GABAergic mechanisms within a distinct posterior insula subarea of freely moving rats, they evoked either analgesia by general GABAergic mediated down regulation via brainstem areas or hyperalgesia by specific $GABA_B$ receptor mediated amygdala projections. In this vein, further evidence is given by studies examining the link between animal (chronic) orofacial pain models and GABA alterations in the TBSNC, indicating generally reduced GABA levels within these pathological conditions (Idänpään-Heikkilä and Guilbaud, 1999, Sessle, 2000; Takemura et al., 2001; Viggiano et al., 2004; Martin et al., 2010; Takeda et al., 2011). Also, a recent animal study by François et al. (2017) proposed a crucial role of GABAergic neurons, however, within the rostral ventromedial medulla (RVM) in integrating sensory inputs together with internal state information, which finally leads to a gatekeeper function for mechanically evoked pain. They further suggest "that multiple parallel GABAergic systems may exist for independent descending control of distinct somatosensory modalities".

In addition to evidence provided by animal research, human resting-state and functional ^{1}H-MRS studies suggest GABA involvement in clinical and acute experimental pain conditions. Henderson et al. (2013) examined GABA resting-state concentrations in the thalamus of patients with painful trigeminal neuropathy (PTN, a form of chronic orofacial pain) compared to healthy volunteers and found significant GABA decreases in patients only. Additionally, they measured volumetric gray matter reductions in the thalamus of PTN patients but not in controls. In our opinion, a conclusive interpretation of their findings as either chronic pain related down-regulated GABAergic neurotransmission or neuronal loss including GABAergic neurons is challenging and needs further investigation. More closely related to our study is the experiment performed by Cleve et al. (2015). Experimental thermal pain was administered to healthy volunteers and GABA alterations in the anterior cingulate and occipital cortex were quantified. In accordance with our results, they observed a GABA associated significant mean

drop of 15.1% during pain stimulation (we observed a drop of 10.88%). They argued that the observed drops could reflect a down-regulation of inhibitory neurotransmission associated with neuro-regulatory processes. Opposed to Cleve et al. and to the study presented here, Kupers et al. (2009) compared neurochemical alterations in the pregenual anterior cingulate cortex associated with tonic heat stimulation and found increases in GABA concentration. A reason for this discrepancy could be rooted in the different regions examined as well as the variety of MRS-sequences applied. Likely most important are differences in the type of pain stimulus and application site used: As we and Cleve et al. (2015) applied a repetitive short phasic stimulus, Kupers et al. utilized tonic heat lasting throughout the whole MRS measurement. It is highly probable that different neurochemical pain processing dynamics are engaged in the measured regions, especially considering the functional diversity of brainstem compared to insular/cingulate/frontal areas.

Despite robust evidence provided for GABA involvement in neurophysiologic and pathologic pain processing (derived from animal and human studies), the question still remains about which underlying neuronal processes may have given rise to the observed reduction in GABA in our study. First of all, the GABA-signal obtained by means of ^{1}H-MRS reflects all GABA in a defined voxel. Therefore, it is not possible to directly ascribe our observed concentration changes to specific GABA pools such as metabolic, vesicular and extrasynaptic compartments (GABA distributed in the extracellular fluid) (Stagg et al., 2011a). Also considerable is the fact that some of the pools are more tightly bound to macromolecules, thus reducing their contribution to the acquired GABA-signal (Stagg et al., 2011a). Animal ^{1}H-MRS studies further suggest that the GABA-signal predominately reflects extrasynaptic GABA (which binds to extrasynaptic $GABA_A$ receptors) and therefore determines a general non-synaptic GABAergic tone (Stagg et al., 2011b). It is also important to mention that levels of measured GABA are not simplistically linked to excitatory activity and that an increase in GABA concentration does not necessarily correspond to increased neuronal inhibition (Rae, 2014). It has generally been proposed that overall GABA levels rather reflect a gross GABAergic tone instead of specific inhibitory activity per se. In that vein, the GABA reduction observed in our study does not need to directly mirror increases in excitatory neurotransmission within the TBSNC due to nociceptive processing (coupled with glutamatergic excitatory neurotransmission). The applied dental stimuli were of 1 ms duration giving rise to associated short dental pain perceptions. In case of induced GABAergic neurotransmission, potentially released GABA into the synaptic cleft would probably be quickly taken up by astrocytes and neurons due to the short stimulation applied. Considering the timespan between excitation of

the MRS volume until the end of the signal readout of approx. 572 ms, it is rather unlikely that such short neurotransmittory processes are measurable with the applied ^{1}H-MRS sequence. In this view, the presented results correspond to the view that the observed decrease in GABA levels may reflect changes in a general GABAergic tone rather than specific and direct GABAergic neurotransmission.

Limitations:

Several limitations need to be considered. Starting with the voxel placement, measuring the TBSNC with ideal anatomical and functional specificity proved to be highly demanding. This circumstance is attributable to the shape of the TBSNC and brainstem in general impeding measurability accuracy using the available cuboid voxel shape. Higher anatomical specificity might be attainable by applying other specificity enhancement strategies currently under development and partly applicable, like the use of arbitrary voxel shapes. This technique enables an exact drawing of the region of interest according to its structural contours thus theoretically achieving higher levels of spatial selectivity (Weber-Fahr et al., 2009; Snyder et al., 2012). However, the lack of contrast of structural MRI in the brainstem hampers the visual identification of TBSNC structures. This circumstance further aggravates the achievement of optimal specificity and resulting increase of sensitivity to neurochemical processes in the TBSNC.

The exclusive assessment of the neurochemical milieu of the TBSNC ipsilateral to the stimulated tooth could represent a further limitation. An additional measurement of the contralateral TBSNC in rest and during dental stimulation could provide valuable insights regarding the lateralization specificity of the observed neurochemical alterations. In the same vein, an additional recovery phase after the pain condition could provide further information on the dynamics of the recorded neurochemical effects. Such examinations are planned.

A possible limitation could be rooted in the exclusive participation of healthy male volunteers. The testing of a female population may demand an adaptation of voxel dimensions due to different brain sizes thus impeding a generalization of our results to the female population and further studies might be necessary.

Further on, we would like to comprehensively address possible limitations regarding the observed changes in GABA.

At 3 Tesla, detection and quantification of GABA is challenging as the signal significantly overlaps with resonances from other neurochemicals. Several approaches have been developed to improve the quantification of GABA at this field strength (Mescher et al., 1998; Schulte and Boesiger, 2006; Stagg, 2013). The most commonly and widely accepted gold-standard of GABA quantification at 3 Tesla is a spectral editing technique named MEGA-PRESS. This method allows the separation of the $^{4}CH_2$-GABA multiplet from the overlapping resonances (Mescher et al., 1998). MEGA-PRESS is a two-step approach which requires the acquisition of "on and off" spectra to calculate the edited spectrum. To date, with respect to our paradigm and the neurochemical quantification within the TBSNC, this method is not applicable due to required voxels sizes and measurement time (high volunteer stress).

Another technique able to improve GABA quantification is 2D *J*-resolved MRS in combination with two-dimensional fitting procedures (Schulte and Boesiger, 2006; Stagg, 2013). However, this approach is also limited within the frame of the present study as significantly larger voxel sizes and longer scan times are required to achieve sufficient SNR.

In this report, MRS sequences and post-processing techniques are based on spinal cord MRS Hock et al., 2013; Hock et al., 2013a; Hock et al., 2016) and are optimized for quantification of neurochemical profiles in the TBSNC. Although methodological work suggests that unedited short-TE MRS measurements at 3 Tesla can yield relatively reliable GABA quantification, distinct caution must be applied regarding the spectral quality between conditions, as differences in linewidth and SNR systematically bias GABA quantification and fitting error estimates (Near et al., 2013). In that sense, special care was applied to ensure comparable spectral quality estimates (linewidth and SNR) between the baseline and pain condition, hence minimizing systematic quantification biases between both conditions (reported in table 1). Another consequence of the resonance overlaps from GABA and other neurochemicals are increased GABA fitting errors. As rule of thumb, neurochemicals determined with CRLB < 20-30% are not considered unreliable, but should be interpreted with caution (De Graaf, 2007). Although mean CRLB for GABA in both conditions meet this criterion, it is important to emphasize that CRLB only reflect lower bounds and therefore may underestimate the actual magnitude of fitting errors. To overcome mentioned limitations we are working on the adaptation of the metabolic cycling technique for the use at 7 Tesla. Additionally, we are working on optimized coil designs to maximize SNR as successfully shown for the spinal cord (Hock et al., 2016).

Conclusion

Conceptualized as a feasibility study, this ^{1}H-MRS investigation provides first evidence of neurochemical alterations in the human TBSNC during experimental orofacial pain. Yet, the findings need to be cautiously interpreted, replication as well as expanding the research focus is indispensable.

We would like to note that the application of ^{1}H-MRS at the level of the TBSNC is possible, allowing the study of neurochemical compositions also in other brainstem subareas. Important in this regard is the measurement quality of tNAA, GABA and the six other quantified neurochemicals (table 1 and 2). Important, since we think that orofacial pain is mediated not only by tNAA and GABA. We rather hypothesize that the general neurochemical composition is somehow involved to code all complex intertwined facets of the human neural pain circuits. This has to be explored in following studies.

This study provides first indications of human brainstem neurochemical nociceptive mechanisms. Hence, it complements identified neurochemical aberrations in animal models of acute/chronic orofacial pain. Thus, bridging both research fields might be in reach and offers hope for successful new treatment opportunities.

Acknowledgements:

This study was funded by the Olga-Mayenfisch science foundation.

References

Baslow, M.H. (2002). Evidence supporting a role for N-acetyl-L-aspartate as a molecular water pump in myelinated neurons in the central nervous system. An analytical review. Neurochemistry international *40*, 295–300.

Baslow, M.H., Cain, C.K., Sears, R., Wilson, D.A., Bachman, A., Gerum, S., and Guilfoyle, D.N. (2016). Stimulation-induced transient changes in neuronal activity, blood flow and N-acetylaspartate content in rat prefrontal cortex: a chemogenetic fMRS-BOLD study. NMR in biomedicine *29*, 1678–1687.

Baslow, M.H., Hrabe, J., and Guilfoyle, D.N. (2007). Dynamic Relationship Between Neurostimulation and N-Acetylaspartate Metabolism in the Human Visual Cortex. J Mol Neurosci *32*, 235–245.

Beck, F., Brown, D., Christ, B., Kriz, W., Marani, E., Putz, R., Sano, Y., Schiebler, T.H., Zilles, K., Usunoff, K.G., Marani, E., and Schoen, J.H.R. (1997). The Trigeminal System in Man (Springer Berlin Heidelberg: Berlin, Heidelberg).

Beissner, F., and Baudrexel, S. (2014). Investigating the human brainstem with structural and functional MRI. Frontiers in human neuroscience *8*, 116.

Benarroch, E.E. (2008). N-acetylaspartate and N-acetylaspartylglutamate: neurobiology and clinical significance. Neurology *70*, 1353–1357.

Brooks, J.C.W., Faull, O.K., Pattinson, K.T.S., and Jenkinson, M. (2013). Physiological noise in brainstem FMRI. Frontiers in human neuroscience *7*, 623.

Brügger, M., Lutz, K., Brönnimann, B., Meier, M.L., Luechinger, R., Barlow, A., Jäncke, L., and Ettlin, D.A. (2012). Tracing toothache intensity in the brain. Journal of dental research 91, 156–160.

Cleve, M., Gussew, A., and Reichenbach, J.R. (2015). In vivo detection of acute pain-induced changes of GABA+ and Glx in the human brain by using functional 1H MEGA-PRESS MR spectroscopy. NeuroImage *105*, 67–75.

DaSilva, A.F., and DosSantos, M.F. (2012). The role of sensory fiber demography in trigeminal and postherpetic neuralgias. Journal of dental research *91*, 17–24.

DaSilva, A.F., Becerra, L., Makris, N., Strassman, A.M., Gonzalez, R.G., Geatrakis, N., and Borsook, D. (2002). Somatotopic activation in the human trigeminal pain pathway. The Journal of neuroscience : the official journal of the Society for Neuroscience *22*, 8183–8192.

De Graaf, R.A. (2007). In vivo NMR spectroscopy. Principles and techniques (John Wiley & Sons: Chichester, West Sussex, England, Hoboken, NJ).

de Matos, N.M.P., Meier, L., Wyss, M., Meier, D., Gutzeit, A., Ettlin, D.A., and Brügger, M. (2016). Reproducibility of Neurochemical Profile Quantification in Pregenual Cingulate, Anterior Midcingulate, and Bilateral Posterior Insular Subdivisions Measured at 3 Tesla. Frontiers in human neuroscience *10*, 300.

Denk, F., McMahon, S.B., and Tracey, I. (2014). Pain vulnerability: a neurobiological perspective. Nature neuroscience *17*, 192–200.

Dreher, W., and Leibfritz, D. (2005). New method for the simultaneous detection of metabolites and water in localized in vivo 1H nuclear magnetic resonance spectroscopy. Magnetic resonance in medicine *54*, 190–195.

Dubner, R., and Bennett, G.J. (1983). Spinal and trigeminal mechanisms of nociception. Annual review of neuroscience *6*, 381–418.

Edden, R.A.E., Schär, M., Hillis, A.E., and Barker, P.B. (2006). Optimized detection of lactate at high fields using inner volume saturation. Magnetic resonance in medicine *56*, 912–917.

Fairhurst, M., Wiech, K., Dunckley, P., and Tracey, I. (2007). Anticipatory brainstem activity predicts neural processing of pain in humans. Pain *128*, 101–110.

François, A., Low, S.A., Sypek, E.I., Christensen, A.J., Sotoudeh, C., Beier, K.T., Ramakrishnan, C., Ritola, K.D., Sharif-Naeini, R., Deisseroth, K., Delp, S.L., Malenka, R.C., Luo, L., Hantman, A.W., and Scherrer, G. (2017). A Brainstem-Spinal Cord Inhibitory Circuit for Mechanical Pain Modulation by GABA and Enkephalins. Neuron *93*, 822-839.e6.

Gussew, A., Rzanny, R., Erdtel, M., Scholle, H.C., Kaiser, W.A., Mentzel, H.J., and Reichenbach, J.R. (2010). Time-resolved functional 1H MR spectroscopic detection of glutamate concentration changes in the brain during acute heat pain stimulation. NeuroImage *49*, 1895–1902.

Gussew, A., Rzanny, R., Güllmar, D., Scholle, H.-C., and Reichenbach, J.R. (2011). 1H-MR spectroscopic detection of metabolic changes in pain processing brain regions in the presence of non-specific chronic low back pain. NeuroImage *54*, 1315–1323.

Gustin, S.M., Peck, C.C., Wilcox, S.L., Nash, P.G., Murray, G.M., and Henderson, L.A. (2011). Different pain, different brain: thalamic anatomy in neuropathic and non-neuropathic chronic pain syndromes. The Journal of neuroscience : the official journal of the Society for Neuroscience *31*, 5956–5964.

Gutzeit, A., Meier, D., Froehlich, J.M., Hergan, K., Kos, S., Weymarn, C., Lutz, K., Ettlin, D., Binkert, C.A., Mutschler, J., Sartoretti-Schefer, S., and Brügger, M. (2013). Differential NMR spectroscopy reactions of anterior/posterior and right/left insular subdivisions due to acute dental pain. European radiology *23*, 450–460.

Gutzeit, A., Meier, D., Meier, M.L., Weymarn, C. von, Ettlin, D.A., Graf, N., Froehlich, J.M., Binkert, C.A., and Brügger, M. (2011). Insula-specific responses induced by dental pain. A proton magnetic resonance spectroscopy study. European radiology *21*, 807–815.

Henderson, L.A., Peck, C.C., Petersen, E.T., Rae, C.D., Youssef, A.M., Reeves, J.M., Wilcox, S.L., Akhter, R., Murray, G.M., and Gustin, S.M. (2013). Chronic pain: lost inhibition? The Journal of neuroscience : the official journal of the Society for Neuroscience *33*, 7574–7582.

Hock, A., and Henning, A. (2016). Motion correction and frequency stabilization for MRS of the human spinal cord. NMR in biomedicine 29, 490–498.

Hock, A., Henning, A., Boesiger, P., and Kollias, S.S. (2013a). (1)H-MR spectroscopy in the human spinal cord. AJNR. American journal of neuroradiology 34, 1682–1689.

Hock, A., MacMillan, E.L., Fuchs, A., Kreis, R., Boesiger, P., Kollias, S.S., and Henning, A. (2013). Non-water-suppressed proton MR spectroscopy improves spectral quality in the human spinal cord. Magnetic resonance in medicine *69*, 1253–1260.

Hurley, R.A., Flashman, L.A., Chow, T.W., and Taber, K.H. (2010). The brainstem: anatomy, assessment, and clinical syndromes. The Journal of neuropsychiatry and clinical neurosciences *22*, iv, 1-7.

Idänpään-Heikkilä, J.J., and Guilbaud, G. (1999). Pharmacological studies on a rat model of trigeminal neuropathic pain: baclofen, but not carbamazepine, morphine or tricyclic antidepressants, attenuates the allodynia-like behaviour. Pain *79*, 281–290.

Jasmin, L., Rabkin, S.D., Granato, A., Boudah, A., and Ohara, P.T. (2003). Analgesia and hyperalgesia from GABA-mediated modulation of the cerebral cortex. Nature *424*, 316–320.

Kreis, R. (2004). Issues of spectral quality in clinical 1H-magnetic resonance spectroscopy and a gallery of artifacts. NMR in biomedicine *17*, 361–381.

Kupers, R., Danielsen, E.R., Kehlet, H., Christensen, R., and Thomsen, C. (2009). Painful tonic heat stimulation induces GABA accumulation in the prefrontal cortex in man. Pain *142*, 89–93.

Lodder-Gadaczek, J., Becker, I., Gieselmann, V., Wang-Eckhardt, L., and Eckhardt, M. (2011). N-acetylaspartylglutamate synthetase II synthesizes N-acetylaspartylglutamylglutamate. The Journal of biological chemistry *286*, 16693–16706.

Maixner, W., Diatchenko, L., Dubner, R., Fillingim, R.B., Greenspan, J.D., Knott, C., Ohrbach, R., Weir, B., and Slade, G.D. (2011). Orofacial pain prospective evaluation and risk assessment study--the OPPERA study. The journal of pain : official journal of the American Pain Society *12*, T4-11.e1-2.

Mangia, S., Tkác, I., Gruetter, R., Van De Moortele, Pierre-Francois, Maraviglia, B., and Uğurbil, K. (2007). Sustained neuronal activation raises oxidative metabolism to a new steady-state level: evidence from 1H NMR spectroscopy in the human visual cortex. Journal of cerebral blood flow and metabolism : official journal of the International Society of Cerebral Blood Flow and Metabolism *27*, 1055–1063.

Martin, Y.B., Malmierca, E., Avendaño, C., and Nuñez, A. (2010). Neuronal disinhibition in the trigeminal nucleus caudalis in a model of chronic neuropathic pain. The European journal of neuroscience *32*, 399–408.

Mescher, M., Merkle, H., Kirsch, J., Garwood, M., and Gruetter, R. (1998). Simultaneous in vivo spectral editing and water suppression. NMR in biomedicine 11, 266–272.

Miyake, M., Kakimoto, Y., and Sorimachi, M. (1981). A gas chromatographic method for the determination of N-acetyl-L-aspartic acid, N-acetyl-alpha-aspartylglutamic acid and beta-citryl-L-glutamic acid and their distributions in the brain and other organs of various species of animals. Journal of neurochemistry *36*, 804–810.

Moffett, J.R., and Namboodiri, A.M.A. (2006). Expression of N-acetylaspartate and N-acetylaspartylglutamate in the nervous system. Advances in experimental medicine and biology *576*, 7-26; discussion 361-3.

Moffett, J.R., Ross, B., Arun, P., Madhavarao, C.N., and Namboodiri, A.M.A. (2007). N-Acetylaspartate in the CNS: from neurodiagnostics to neurobiology. Progress in neurobiology *81*, 89–131.

Mullins, P.G., Rowland, L.M., Jung, R.E., and Sibbitt, W.L. (2005). A novel technique to study the brain's response to pain: proton magnetic resonance spectroscopy. NeuroImage *26*, 642–646.

Murray, C.J.L., and Lopez, A.D. (2013). Measuring the global burden of disease. The New England journal of medicine *369*, 448–457.

Near, J., Andersson, J., Maron, E., Mekle, R., Gruetter, R., Cowen, P., and Jezzard, P. (2013). Unedited in vivo detection and quantification of γ-aminobutyric acid in the occipital cortex using short-TE MRS at 3 T. NMR in biomedicine 26, 1353–1362.

Nieuwenhuys, R., Voogd, J., and van Huijzen, C. (2008). The human central nervous system (Springer: Berlin, New York).

Peyron, R., Laurent, B., and García-Larrea, L. (2000). Functional imaging of brain responses to pain. A review and meta-analysis (2000). Neurophysiologie Clinique/Clinical Neurophysiology *30*, 263–288.

Provencher, S.W. (1993). Estimation of metabolite concentrations from localized in vivo proton NMR spectra. Magnetic resonance in medicine *30*, 672–679.

Rae, C.D. (2014). A guide to the metabolic pathways and function of metabolites observed in human brain 1H magnetic resonance spectra. Neurochemical research *39*, 1–36.

Schulte, R.F., and Boesiger, P. (2006). ProFit. Two-dimensional prior-knowledge fitting of J-resolved spectra. NMR in biomedicine 19, 255–263.

Sessle, B.J. (2000). Acute and chronic craniofacial pain: brainstem mechanisms of nociceptive transmission and neuroplasticity, and their clinical correlates. Critical reviews in oral biology and medicine : an official publication of the American Association of Oral Biologists *11*, 57–91.

Sessle, B.J. (2005). Peripheral and central mechanisms of orofacial pain and their clinical correlates. Minerva anestesiologica *71*, 117–136.

Slusher, B.S., Tsai, G., Yoo, G., and Coyle, J.T. (1992). Immunocytochemical localization of the N-acetyl-aspartyl-glutamate (NAAG) hydrolyzing enzyme N-acetylated alpha-linked acidic dipeptidase (NAALADase). The Journal of comparative neurology *315*, 217–229.

Smith, S.A., Levante, T.O., Meier, B.H., and Ernst, R.R. (1994). Computer Simulations in Magnetic Resonance. An Object-Oriented Programming Approach. Journal of Magnetic Resonance, Series A *106*, 75–105.

Snyder, J., Haas, M., Dragonu, I., Hennig, J., and Zaitsev, M. (2012). Three-dimensional arbitrary voxel shapes in spectroscopy with submillisecond TEs. NMR in biomedicine 25, 1000–1006.

Stagg, C.J. (2013). Magnetic resonance spectroscopy. Tools for neuroscience research and emerging clinical applications (Academic Press: Amsterdam).

Stagg, C.J., Bachtiar, V., and Johansen-Berg, H. (2011a). What are we measuring with GABA magnetic resonance spectroscopy? Communicative & integrative biology *4*, 573–575.

Stagg, C.J., Bestmann, S., Constantinescu, A.O., Moreno, L.M., Allman, C., Mekle, R., Woolrich, M., Near, J., Johansen-Berg, H., and Rothwell, J.C. (2011b). Relationship between physiological measures of excitability and levels of glutamate and GABA in the human motor cortex. The Journal of physiology *589*, 5845–5855.

Takeda, M., Matsumoto, S., Sessle, B.J., Shinoda, M., and Iwata, K. (2011). Peripheral and Central Mechanisms of Trigeminal Neuropathic and Inflammatory Pain. Journal of Oral Biosciences *53*, 318–329.

Takemura, M., Shimada, T., and Shigenaga, Y. (2001). GABA B receptor-mediated effects on expression of c-Fos in rat trigeminal nucleus following high- and low-intensity afferent stimulation. Neuroscience *103*, 1051–1058.

Tallan, H.H. (1957). Studies on the distribution of N-acetyl-L-aspartic acid in brain. The Journal of biological chemistry *224*, 41–45.

Tang, F.R., Yeo, J.F., and Leong, S.K. (2001). Qualitative light and electron microscope study of glutamate receptors in the caudal spinal trigeminal nucleus of the rat. Journal of dental research *80*, 1736–1741.

Tranberg, M., Stridh, M.H., Guy, Y., Jilderos, B., Wigström, H., Weber, S.G., and Sandberg, M. (2004). NMDA-receptor mediated efflux of N-acetylaspartate: physiological and/or pathological importance? Neurochemistry international *45*, 1195–1204.

Truckenmiller, M.E., Namboodiri, M.A.A., Brownstein, M.J., and Neale, J.H. (1985). N-Acetylation of L-Aspartate in the Nervous System: Differential Distribution of a Specific Enzyme. J Neurochem *45*, 1658–1662.

Viggiano, A., Monda, M., Viggiano, A., Chiefari, M., Aurilio, C., and Luca, B. de (2004). Evidence that GABAergic neurons in the spinal trigeminal nucleus are involved in the transmission of inflammatory pain in the rat: a microdialysis and pharmacological study. European journal of pharmacology *496*, 87–92.

Wager, T.D., Atlas, L.Y., Lindquist, M.A., Roy, M., Woo, C.W., and Kross, E. (2013). An fMRI-based neurologic signature of physical pain. The New England journal of medicine *368*, 1388–1397.

Weber-Fahr, W., Busch, M.G., and Finsterbusch, J. (2009). Short-echo-time magnetic resonance spectroscopy of single voxel with arbitrary shape in the living human brain using segmented two-dimensional selective radiofrequency excitations based on a blipped-planar trajectory. Magn Reson Imaging 27, 664–671.

Wiesenfeld-Hallin, Z. (2005). Sex differences in pain perception. Gender Medicine *2*, 137–145.

Wilcox, S.L., Gustin, S.M., Macey, P.M., Peck, C.C., Murray, G.M., and Henderson, L.A. (2015). Anatomical changes within the medullary dorsal horn in chronic temporomandibular disorder pain. NeuroImage *117*, 258–266.

Yamada, T., Zuo, D., Yamamoto, T., Olszewski, R.T., Bzdega, T., Moffett, J.R., and Neale, J.H. (2012). NAAG peptidase inhibition in the periaqueductal gray and rostral ventromedial medulla reduces flinching in the formalin model of inflammation. Molecular pain *8*, 67.

Zakrzewska, J.M. (2013). Multi-dimensionality of chronic pain of the oral cavity and face. The journal of headache and pain *14*, 37.

Zhang, W., Murakawa, Y., Wozniak, K.M., Slusher, B., and Sima, A A F (2006). The preventive and therapeutic effects of GCPII (NAALADase) inhibition on painful and sensory diabetic neuropathy. Journal of the neurological sciences *247*, 217–223.

Zhang, W., Slusher, B., Murakawa, Y., Wozniak, K., Tsukamoto, T., Jackson, P., and Sima, A. (2002). GCPII (NAALADase) inhibition prevents long-term diabetic neuropathy in type 1 diabetic BB/Wor rats. Journal of the neurological sciences *194*, 21–28.

Zhao, J., Ramadan, E., Cappiello, M., Wroblewska, B., Bzdega, T., and Neale, J.H. (2001). NAAG inhibits KCl-induced [(3)H]-GABA release via mGluR3, cAMP, PKA and L-type calcium conductance. The European journal of neuroscience *13*, 340–346.

Zhong, C., Zhao, X., Van, K.C., Bzdega, T., Smyth, A., Zhou, J., Kozikowski, A.P., Jiang, J., O'Connor, W.T., Berman, R.F., Neale, J.H., and Lyeth, B.G. (2006). NAAG peptidase inhibitor increases dialysate NAAG and reduces glutamate, aspartate and GABA levels in the dorsal hippocampus following fluid percussion injury in the rat. Journal of neurochemistry *97*, 1015–1025.